

International Journal of Scientific Research and Reviews

A 3D Model for Thickness and Diffusion Capacitance of Emitter-Base Junction Determination in A Monofacial Polycrystalline Solar Cell under Real Operating Condition

¹Mayoro Dieye*, ^{1,2}Awa Dieye and ^{1,2}Nacire Mbengue

¹Solar Energy Materials and Systems Laboratory (LASES), University cheikh anta diop of Dakar (UCAD), department of physic, science faculty, BP: 5005

²Semiconductor Optoelectronics Group (GOES), University cheikh anta diop of Dakar (UCAD), department of physic, science faculty, BP: 5005

ABSTRACT

The purpose of this study is to show the effect of irradiation on the relative density of minority charge carriers and space charge region extension of a three-dimensional polycrystalline silicon bifacial photopile under multispectral illumination in the static regime. Solving the continuity equation allowed us to determine the expression of the excess minority charge carrier density. From this density, the expression of the relative density is deduced and studied as a function of the irradiation energy and the damage coefficient. The study showed that the thickness of the space charge zone decreases with increasing irradiation energy and damage coefficient.

KEYWORDS: Photocell -Irradiation -Scattering capacity-Recombination rate at grain boundaries- Grain size, polycrystalline.

***Corresponding author**

Dr. Mayoro DIEYE

Departement of physic
Solar Energy Materials and Systems Lab (LASES)
University Cheikh anta diop of dakar, BP : 5005
Science faculty

1. INTRODUCTION

Several techniques of characterization of the silicon material, determination of the phenomenological and electrical parameters have been used to improve the capacity of solar cells. Some of these techniques have been developed in static regime¹ and others in dynamic frequency regime². Extensive studies on the capacity of the space charge area^{3,5}, have been carried out in 3 dimensions^{1,5,8} for these two regimes. When the photocell is illuminated, we witness a storage of opposite charges on both sides of the emitter-base junction. This leads to the establishment of a planar capacitor whose capacity varies according to the recombination rate at the junction, the irradiation energy and the damage coefficient. Thus, the diffusion capacitance has been the subject of several studies in the static regime in order to determine the doping rate^{9,10}. In the transient regime, the extension of the space charge zone is obtained^{11,12}. In the dynamic frequency regime, the volume and surface recombination parameters are sought^{13,14}. Indeed, when there is an important absorption of irradiation, the concentration of electrons and holes are modified and the parameters of solar cells are strongly modified¹⁵. Our contribution consists in determining the relative density and the extension of the space charge zone of a three-dimensional silicon solar cell in static regime under irradiation and multispectral illumination.

We briefly present a theoretical study in which we schematize a grain of the photopile and solve the diffusion equation. Then we discuss the results obtained before concluding.

2. MODELING AND THEORETICAL ANALYSIS

As a n+ -p-p+ polycrystalline solar cell¹⁶ is made of many small individual grains, grain boundary effects are important; an example being grain boundaries act as electron-hole traps.

With regard to physical process simulation, we can consider the fibrously oriented columnar grain as shown in Figure 1 in cross-section, Figure 2 illustrates the bifacial solar cell in a planar configuration. Considering an isolated grain in Figure 3, we made calculations in order to study the variation of the main parameters, such as grain size g , grain boundaries recombination velocity S_{gb} , irradiation (KI, ϕ) and illumination modes.

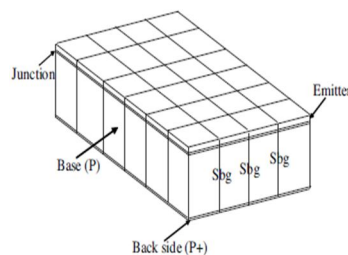


Figure1: Fibrously oriented

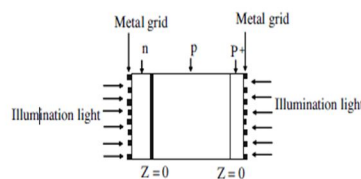


Figure 2: Bifacial solar cell

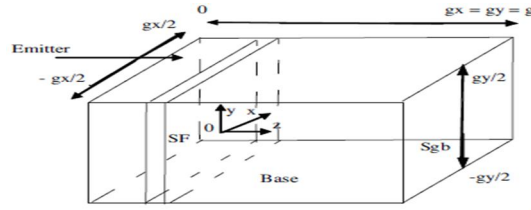


Figure 3: Schematic of an isolated grain

Excess Minority Carriers Density

Considering the emitter as a dead (non active) area, the excess minority carrier distribution in the base, seen as a greater contribution to the photo-conversion, is derived from the continuity equations^{5,11}:

$$D(Kl, \phi) \times \left[\frac{\partial^2 \delta(x, y, z)}{\partial x^2} + \frac{\partial^2 \delta(x, y, z)}{\partial y^2} + \frac{\partial^2 \delta(x, y, z)}{\partial z^2} \right] - \frac{\delta(x, y, z)}{\tau} + G(z) = 0 \quad (1)$$

$D(Kl, \phi)$ is the diffusion coefficient in the presence of irradiation.

It is expressed as follows:

$$D(Kl, \phi) = \frac{L(Kl, \phi)^2}{\tau} \quad (2)$$

In this expression, $G(z)$ represents the generation rate of minority charge carriers in the base²⁵ whose expression is given by the following equation :

$$G(z) = \sum_{i=1}^3 a_i \times \exp(-b_i \times z) \quad (3)$$

Les valeurs a_i et b_i sont les valeurs tabulées à partir de la modélisation du spectre d'absorption de la photopile pour AM 1.5^{10,16,17}.

L depend on the irradiation energy Φ and the damage coefficient Kl through the following expressions^{26,28}:

$$L(Kl, \phi) = \sqrt{\frac{1}{\frac{1}{L_0^2} + Kl \times \phi}} \quad (4)$$

L_0 is the diffusion length without irradiation.

The solution of the equations can be written as follows The solution of the equations can be written as follows^{5,17,18} :

$$\delta(x, y, z) = \sum_k \sum_j Z_{k,j}(z) \times \cos(C_k \times x) \times \cos(C_j \times y) \quad (5)$$

k, j : are the indices for the x and y directions respectively.

C_k and C_j are obtained from the conditions at the grain boundaries^{5,18,22,23} $\pm \frac{g_x}{2}$ et $\pm \frac{g_y}{2}$.

$$\left[\frac{\partial \delta(x, y, z)}{\partial x} \right]_{x=\pm \frac{g_x}{2}} = \mu \frac{Sgb}{D(Kl, \phi)} \delta\left(\pm \frac{g_x}{2}, y, z\right) \quad (6)$$

$$\left[\frac{\partial \delta(x, y, z)}{\partial y} \right]_{y=\pm \frac{g_y}{2}} = \mu \frac{Sgb}{D(Kl, \phi)} \delta\left(x \pm \frac{g_y}{2}, z\right) \quad (7)$$

g_x is the grain width, g_y the grain length Sgb the recombination velocity at the grain boundaries.

From equations 6 and 7 we obtain two transcendental equations²⁹ which are:

$$\tan\left(C_k \times \frac{g_x}{2}\right) = \frac{Sgb}{2.C_k \times D(Kl, \phi)} \quad (8)$$

$$\tan\left(C_j \times \frac{g_y}{2}\right) = \frac{Sgb}{2.C_j \times D(Kl, \phi)} \quad (9)$$

By replacing $\delta(x, y, z)$ in the continuity equation and the fact that the cosine function is orthogonal, we obtain the following differential equation:

$$Z_{k,j} = A_{k,j} \times \cosh\left(\frac{z}{L_{k,j}}\right) + B_{k,j} \times \sinh\left(\frac{z}{L_{k,j}}\right) - \sum_{i=1}^3 K_{i,j,k} \times \exp(-b_i \times z) \quad (10)$$

Or

$$K_{i,j,k} = \frac{L_{k,j}^2}{D_{k,j} \times [b_i^2 \times L_{k,j}^2 - 1]} \times a_i \quad (11)$$

$$\text{With } L_{k,j} = \left[C_k^2 + C_j^2 + \frac{1}{L(Kl, \phi)^2} \right]^{\frac{1}{2}} \quad (12)$$

And

$$D_{k,j} = D(Kl, \phi) \times \frac{[C_k \times g_x + \sin(C_k \times g_x)][C_j \times g_y + \sin(C_j \times g_y)]}{16. \sin\left(C_k \times \frac{g_x}{2}\right). \sin\left(C_j \times \frac{g_y}{2}\right)} \quad (13)$$

The coefficients $A_{k,j}$ and $B_{k,j}$ are calculated from the following boundary conditions^{5,19,20}:

At the junction ($z = 0$ $z = 0$):

$$\left[\frac{\partial \delta(x, y, z)}{\partial z} \right]_{z=0} = \frac{Sf}{D(Kl, \phi)} \delta(x, y, 0) \quad (14)$$

Sf is the junction recombination velocity, written as $Sf = Sf_0 + Sf_j$ with Sf_0 being the intrinsic junction recombination velocity related to the shunt resistance due to losses occurring across the junction and Sf_j is the imposed junction recombination velocity due external load. It defines the current flow that is the operating point of the cell. For each illumination mode, the intrinsic junction recombination velocity was calculated using the method described in^{5,8,19,20,24}.

At the back side ($z = \omega b$):

$$\left[\frac{\partial \delta(x, y, z)}{\partial z} \right]_{z=0} = -\frac{Sb}{D(Kl, \phi)} \delta(x, y, \omega b) \quad (15)$$

Sb is the back surface recombination velocity. It quantifies the rate at which excess minority carriers are lost at the back surface of the cell. The derivation of the photocurrent with respect to Sf, provides for each illumination mode the expression of Sb, as in^{5,8,19,20,24}.

$$A_{k,j} = \sum_{i=1}^3 K_{i,k,j} \times \frac{\frac{1}{L_{k,j}} \left(\frac{Sf}{D(Kl, \phi)} - b_i \right) \times \exp(-b_i \times \omega b) + Y_{k,j} \left(\frac{Sf}{D(Kl, \phi)} + b_i \right)}{\frac{Sf \times Y_{k,j}}{D(Kl, \phi)} + \frac{X_{k,j}}{L_{k,j}}} \quad (16)$$

$$B_{k,j} = \sum_{i=1}^3 K_{i,k,j} \times \frac{\frac{Sf}{D(Kl, \phi)} \left(\frac{Sb}{D(Kl, \phi)} - b_i \right) \times \exp(-b_i \times \omega b) + X_{k,j} \left(\frac{Sf}{D(Kl, \phi)} + b_i \right)}{\frac{Sf \times Y_{k,j}}{D(Kl, \phi)} + \frac{X_{k,j}}{L_{k,j}}} \quad (17)$$

With:

$$X_{k,j} = \frac{1}{L_{k,j}} \times \sinh\left(\frac{\omega b}{L_{k,j}}\right) + \frac{Sb}{D(Kl, \phi)} \times \cosh\left(\frac{\omega b}{L_{k,j}}\right) \quad (18)$$

$$Y_{k,j} = \frac{1}{L_{k,j}} \times \cosh\left(\frac{\omega b}{L_{k,j}}\right) + \frac{Sb}{D(Kl, \phi)} \times \sinh\left(\frac{\omega b}{L_{k,j}}\right) \quad (19)$$

Relative Density of Minority Charge Carriers

We have seen upstream that when the photocell is illuminated by a polychromatic light, there is storage of charges of opposite signs on both sides of the junction and an enlargement of the space charge area. Thus, this junction is comparable to a plane capacitor whose displacement of the armatures produces a current density. This displacement is relative to the operating point and to the variation of the maximum density point of the minority charge carriers in excess in the base.

We will now study the relative density of the excess minority charge carriers in the base which is defined as follows:

$$\delta_{rel}(z, Sf, Sb, g, Sgb, Kl, \phi) = \frac{\delta(z, Sf, Sb, g, Sgb, Kl, \phi)}{\delta_{max}} \quad (20)$$

δ_{max} is the maximum density of minority charge carriers.

To materialize the displacement of the maximum point of the minority charge carrier density that we present the following Figures (4, 5, 6, 7) which illustrate the profile of the relative density of

minority charge carriers as a function of the depth of the base for different operating points and for different values of the recombination velocities at the S_{fj} junction, grain sizes, recombination velocities at the grain boundaries, irradiation energy, and the damage coefficient.

3. RESULTATS ET DISCUSSIONS

Effect of the grain size on the relative density

In the same wake, we plot in Figures 4 the profile of the relative density of minority charge carriers as a function of depth in the base as the grain size varies.

In this study, we assume that the recombination rate at the joints, the irradiation energy and the damage coefficient are constant.

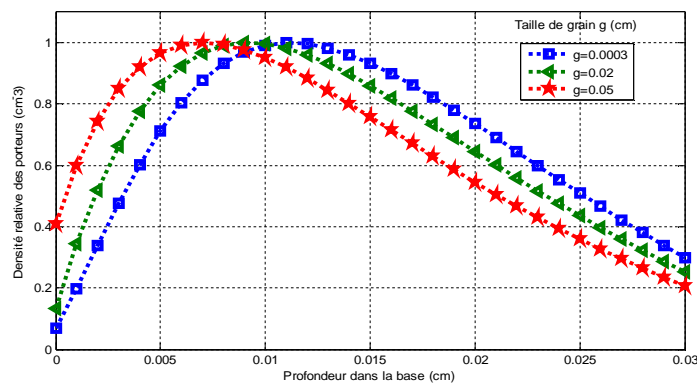


Figure 4: Relative density of minority charge carriers as a function of depth z in the base for different grain sizes $S_{gb}=4,5 \times 10^6 \text{ cm/s}$; $KI=10,5 \text{ cm}^2/\text{MeV}$; $\Phi=150 \text{ MeV}$; $S_{fj}=106 \text{ cm/s}$; $\omega b=0.03 \text{ cm}$ and AM 1.5

We can see on this Figure 4 that the density of minority charge carriers always increases with the grain size as underlined earlier, but we have here in the case of illumination by the front face a shift of the maximum of carriers. More precisely, we observe a displacement of the maximum of charge carriers towards the junction, i.e. a narrowing of the space charge zone.

Effect of recombination velocity at S_{gb} grain boundaries on relative density

Thus, in Figure 5 below, we present the profile of the relative density of minority charge carriers as a function of depth in the z -base for different recombination velocities at S_{gb} grain boundaries.

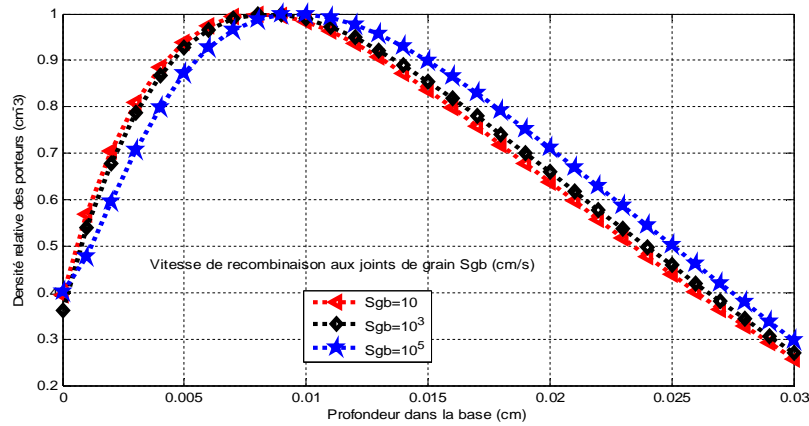


Figure 5: Relative density of minority charge carriers as a function of depth z in the base for a grain size $g = 0.0005\text{cm}$ and for different values of the recombination rate at the junction $Kl=10,5\text{ cm}^{-2}/\text{MeV}$; $\Phi=150\text{ MeV}$; $S_{fj}=5.105\text{cm/s}$, $\omega b=0.03\text{ cm}$ and AM 1.5

The above curve allows us to better perceive the influence of the recombination velocity at the grain boundary; we can indeed observe a significant decrease in the vicinity of the junction with respect to the amplitude and the carrier gradient. This curve confirms our previous observations concerning the effect of the recombination velocity at the grain boundaries.

We note once again a shift of the charge carrier maximum, but this time a widening of the space charge zone.

The influence of the grain size, of the recombination velocity at the grain boundaries and of the irradiation energy is shown, we propose to see now the effect of the damage coefficient on the relative density of minority charge carriers.

Effect of irradiation energy on the relative density of minority charge carriers

Thus we consider that the grain size, the recombination rate at the grain boundaries and the damage coefficient are constant. This cell under invariant illumination is illuminated from the front.

The Figure 6 shows the effect of the irradiation energy on the relative density of minority charge carriers as a function of the depth z of a front-illuminated photocell.

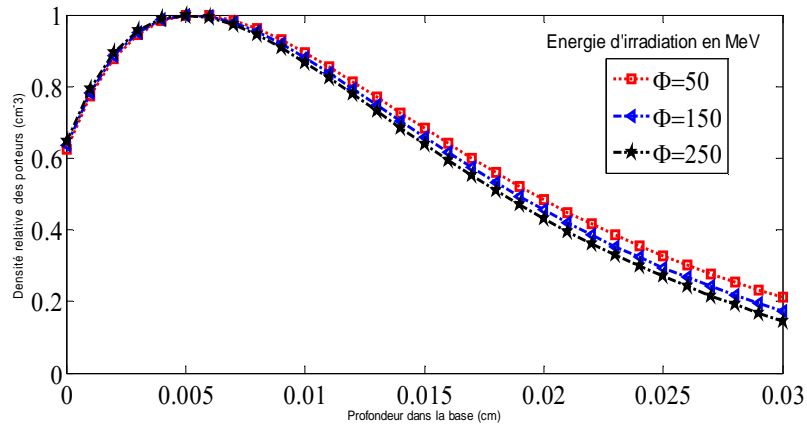


Figure6: Relative density of minority charge carriers as a function of depth z in the base for a grain size g = 0.0005cm and for different irradiation energy values, Sfj=5.105 cm/s; Sgb=4,5x10⁶ cm/s ; Kl=10,5 cm²/MeV; τ=10⁻⁵ s ; ωb=0.03 cm and AM 1.5

We can see on this Figure 6 shows the influence of the irradiation energy with the reduction of the mobility of minority charge carriers at the junction and a decrease in the density of minority charge carriers with the irradiation energy ϕ . This confirms our previous results, but here we have for front side illumination a shift of the charge carrier maximum towards the base.

Effect of the damage coefficient Kl on the relative density

We can also illustrate on the following Figure 7 the profile of the relative density of minority charge carriers as a function of the depth z for different damage coefficients. For this purpose, we will fix the recombination rate at the grain boundaries, the grain size and the irradiation energy.

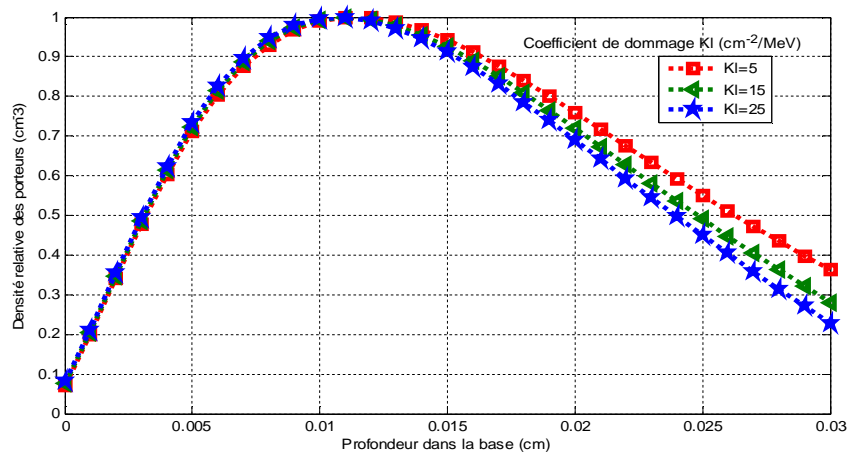


Figure7: Relative density of minority charge carriers as a function of depth z in the base for a grain size g = 0.0005cm and for different damage coefficient values Sfj=5.105 cm/s; Sgb=4,5x10⁶ cm/s ; φ=20MeV; τ=10⁻⁵ s ; ωb=0.03 cm and AM 1.5

In this Figure 7 above, we can see that the space charge region enlargement increases as the damage coefficient increases.

Indeed, one of the consequences of the damage coefficient K_I is to reduce the density of minority charge carriers in the base. Hence an extension of the space charge zone up to its limit value, which corresponds to the enlargement of the latter when the solar cell is operating in short circuit. For this operating regime, the passage of minority charge carriers at the junction leads to a significant expansion of the space charge zone

Moreover, by analyzing the effect of the damage coefficient, we find that there is a slight reduction of the space charge zone when the damage coefficient decreases. Thus, independently of the recombination rate at the grain boundaries, the irradiation energy and the grain size, the thickness of the space charge zone evolves in the same direction as the damage coefficient.

4. CONCLUSION

In this paper we have studied the three-dimensional polycrystalline silicon photocell under irradiation and multispectral illumination from the front side in static regime. This study showed us that the thickness of the space charge region shrinks with the increase of the recombination rate at the junction. With the increase of the irradiation energy and of the damage coefficient, the thickness of the space charge zone widens, hence the decrease of the capacity efficiency of the photopile. The study of the relative densities of the minority charge carriers as a function of the depth z in the base, introduces the extension Z_0 of the space charge zone.

The extension Z_0 , of the space charge zone characterizes the operating point of open-circuit operation of the photopile and its quality.

REFERENCES

1. M.L.Samb, S.Sarr, S.Mbodji, S.Gueye, M.Dieng and G.Sissoko;, Study in 3-D modeling of a silicon photocell in static regime under multispectral illumination multispectral illumination: determination of the electrical parameters. *J. Sci.*, 2009 ; 9, N° 4: 36 – 50. <http://www.cadjds.org>
2. S. Mbodji, A. S. Maïga, M. Dieng, A. Wereme and G. Sissoko; Renoval charge technic applied to a bifacial solar cell under constant magnetic field; *Global journal of pure and applied sciences*, 2010;16, N⁰. 4: 469- 477. <http://www.globaljournalseries.com>

3. S. Madougou, Nzonzolo, S. Mbodji, I.F. Barro and G. Sissoko; Bifacial silicon cell space charge region width determination by a study in modelling: effect of the magnetic field; *J.Sci.* 2004; 4, N°. 3: 116-123. <http://www.cadjds.org>
4. F. I. Barro, S. Mbodji, M. Ndiaye, E. Ba and G. Sissoko; Influence of grains size and grains boundaries recombination on the space-charge layer thickness z of emitter-base junction's n^+-p-p^+ solar cell. Proceedings of the 23rd European Photovoltaic Solar Energy Conference, 2008; 604-607. DOI : 10.4229/23rdEUPVSEC2008-1CV.2.63. <http://www.eupvsec-proceedings.com>
5. H. L. Diallo, A. S. Maïga, A. Wereme, G. Sissoko; New approach of both junction and back surface recombination velocity in a 3D modelling study of a polycrystalline silicon solar cell. *Eur. Phys. J. Appl. Phys.* 2008; 42; 203–211
6. A. Dieng, M.L. Sow, S. Mbodji, M.L. Samb, M. Ndiaye, M. Thiame, F.I. Barro and G. Sissoko; 3D Study of a Polycrystalline Silicon Solar Cell: Influence of Applied Magnetic Field on the Electrical Parameters; Proceedings of the 24th Europea Photovoltaic Solar Energy Conference, 2009; 473-476 DOI: 10.4229/24thEUPVSEC2009- 1CV.4.16. <http://www.eupvsec-proceedings.com>
7. B. Zouma, A. S. Maïga, M. Dieng, F. Zougmore, G. Sissoko; 3D Approach of spectral response for a bifacial silicon solar cell under a constant magnetic field *Global Journal of Pure and Applied Sciences*, 2009;15, N°. 1:117-124. <http://www.globaljournalseries.com>
8. S. Mbodji, M. Dieng, B. Mbow, F. I. Barro and G. Sissoko; , Three dimensional simulated modelling of diffusion capacitance of polycrystalline bifacial silicon solar cell. *Journal of Applied Sciences and Technology (JAST)* 2010; 15, Nos.1&2: 109 –114 <http://www.inasp.info/ajol>
9. A. Jakubowski; Graphic method of substrate doping determination from C-V characteristics of MIS capacitors, *Solid-State Electronics, J. Sci.*, 1981;24, No. 10; 985-987.
10. G. Yaron and D. F.-Bentchkowsky; Capacitance voltage characterization of poly Si-SiO₂-Si structures, *Solid-State Electronics. J. Sci.*, 1980; 23;433-439
11. S. Mbodji, B. Mbow, F. I. Barro and G. Sissoko; A 3D model for thickness and diffusion capacitance of emitter-base junction determination in a bifacial polycrystalline solar cell under real operating condition, *Turkish Journal of Physics*, 2011; 35: 281–291. <http://www.ajol.info/index.php/jast/article/view/54834>
12. E.Sow, S. Mbodji, B. Zouma, M. Zoungrana, I. Zerbo, A. Sere and G. Sissoko; Determination in 3D modeling study of the width emitter extension region of the solar cell

- operating in open circuit condition by the Gauss's Law, International Journal of Science, Environment and Technology (IJSET), 2012; 1, N^o. 4: 331– 34.
13. H. Bayhan, A. S. Kavasoglu; Admittance and impedance spectroscopy on Cu(In,Ga)Se₂ solar cells. Turk. J. Phys., 200327, pp. 529-535.
 14. J. H. Scofield; (1995), Effects of series resistance and inductance on solar admittance measurements, Solar Energy Materials and Solar Cells, J. Sci., 37 (2), pp. 217- 233
 15. I. Gaye , R. Sam , A.D. Seré , I.F. Barro , M.A. Ould El Moujtaba , R. Mané , G Sissoko; (2014), Influence of Irradiation and Damage Coefficient on the Minority Carrier Density in Transient Response for a Bifacial Silicon Solar Cell, Current Trend in Technology and Science, ISSN : 2279-0535. Vol. 3, Issue : 2, pp. 98-104.
 16. J. Oualid and C. M. Singal; (1984), Influence of illumination on the grain boundary recombination velocity in silicon. J. Appl. Phys. 55(4), pp. 1195-1205.
 17. J. Dugas; (1994), 3 D Modelling of a Reverse Cell Made with improved Multycrystalline Silicon Wafers, Solar Energy Materials and Solar Cells, Vol.32, N^o 1, pp.71-88
 18. M .C Halder and T.R.Williams; (1983), Grain boundary effects in polycrystalline Silicon SolarCells I. Solution of the three- Dimensional diffusion equation by the Green's function method, Solar Cells. J. Sci., Vol. 8, N^o 3, pp. 201-22
 19. G. Sissoko, E. Nanéma, A. Corrúa, P. M. Biteye, M. Adj, A. L. Ndiaye; (1998) Silicon Solar cell recombination parameters determination using the characteristic Renewable Energy, Vol-3, pp.1848-1851 Elsevier Science Ltd, 0960-1481/98/#.
 20. G. Sissoko, C. Museruka, A. Correa, I. Gaye, A. L. Ndiaye; (1996), Light spectral effect on recombination parameters of silicon solar cell. In Proceedings of the World Renewable Energy Congress, pp.1487-1490.
 21. M. M. Dione, I. Ly, A. Diao, S. Gueye, A. Gueye, M. Thiame, G. Sissoko; (2013), Determination of the impact of the grain size and the recombination velocity at grain boundary on the values of the electrical parameters of a bifacial polycrystallin silicon sola rcell, IRACST – Engineering Science and Technology: International Journal, Vol.3, N^o .1, pp. 66-73.
 22. Nzonzolo, Lilonga-Boyenga, D., Mabika, C.N. and Sissoko, G.; (2016), Two- Dimensional Finite Element Method Analysis Effect of the Recombination Velocity at the Grain Boundaries on the Characteristics of a Polycrystalline Silicon Solar Cell. Circuits and Systems, Vol. 7, pp.4186-4200 <http://dx.doi.org/10.4236/cs.2016.713344>
 23. S. R. Dhariwal; (1988), Photocurrent and photovoltage from polycrystalline p-n junction solar cells. Solar Cells, Vol. 25, pp. 223-233.

24. M. Ndiaye, A. Diao, M. Thiame, M. M. Dione, H. LY. Diallo, M. L. Samb, I. Ly, Gassama, S. mbodji, F. I. Barro and G. Sissoko; (2010), 3D Approach for a Modelling Study of the Diffusion Capacitance's Efficiency of the Solar Cell; Proceedings of 25 th European Photovoltaic Solar Energy Conference and Exhibition, Valencia, Spain, pp. 484-487.
25. Jose Furlan and Slavko Amon; (1985), Approximation of the carrier generation rate in illuminated silicon, Solid State Electr, Vol. 28, No.12, pp.1241-1243.
26. R. J. Walters and G. P. Summers; (2002), Space Radiation Effects in Advanced Solar Cell Materials and Devices Mat. Res. Soc. Symp. Proc. Vol. 692, pp. 569-580.
27. M. A. Ould El Moujtaba, M. Ndiaye, A. Diao, M. Thiame, I.F. Barro and G. Sissoko; (2012), Theoretical Study of the Influence of Irradiation on a Silicon Solar Cell under Multispectral Illumination. Research Journal of Applied Sciences, Engineering and Technology, 4(23): pp. 5068-5073.
28. R. K. Ahrenkiel, D. J. Dunlavy, H. C. Hamaker, R. T. Green, C. R. Lewis, R. E. Hayes, H. Fardi; (1986), Time-of-flight studies of minority-carrier diffusion in $Al_xGa_{1-x}As$ homojunctions. J. Appl. Phys. 49(12).
29. M. M. Deme, S. Mbodji, S. Ndoeye, A. Thiam, A. Dieng and G. S; (2010), Influence of illumination incidence angle, grain size and grain boundary recombination Velocity on the facial solar cell diffusion capacitance; Revue des Energies Renouvelables Vol. 13 N°1, pp. 109-121.